Virology 393 (2009) 265–271

Contents lists available at ScienceDirect

Virology

journal homepage: www.elsevier.com/locate/yviro

SARS-coronavirus spike S2 domain flanked by cysteine residues C822 and C833 is important for activation of membrane fusion

Ikenna G. Madu, Sandrine Belouzard, Gary R. Whittaker *

C4127 Veterinary Medical Center, Department of Microbiology and Immunology, Cornell University, Ithaca NY 14853, USA

ARTICLE INFO

Article history:
Received 8 May 2009
Returned to author for revision 27 May 2009
Accepted 30 July 2009
Available online 29 August 2009

Keywords:
SARS coronavirus
Spike protein
Membrane fusion
Disulfide loop

ABSTRACT

The S2 domain of the coronavirus spike (S) protein is known to be responsible for mediating membrane fusion. In addition to a well-recognized cleavage site at the S1–S2 boundary, a second proteolytic cleavage site has been identified in the severe acute respiratory syndrome coronavirus (SARS-CoV) S2 domain (R797). C-terminal to this S2 cleavage site is a conserved region flanked by cysteine residues C822 and C833. Here, we investigated the importance of this well conserved region for SARS-CoV S-mediated fusion activation. We show that the residues between C822–C833 are well conserved across all coronaviruses. Mutagenic analysis of SARS-CoV S, combined with cell–cell fusion and pseudotyped virion infectivity assays, showed a critical role for the core-conserved residues C822, D830, L831, and C833. Based on available predictive models, we propose that the conserved domain flanked by cysteines 822 and 833 forms a loop structure that interacts with components of the SARS-CoV S trimer to control the activation of membrane fusion.

Introduction

The severe acute respiratory syndrome coronavirus (SARS-CoV) emerged in 2002 causing a global epidemic. The outbreak resulted in about 8000 cases with a fatality of about 10% until it was quarantined (Drosten et al., 2003; Fouchier et al., 2003). SARS-CoV still maintains a significant threat to human health, as novel viruses such as these still present a possibility for re-emergence into the human population so an understanding of the mechanics of entry is crucial in order to develop effective treatment.

Coronaviruses are enveloped viruses with positive sense RNA genomes that commonly cause respiratory and enteric diseases within a wide host range (Holmes, 2003). Entry of these viruses is mediated by the viral spike glycoprotein S and a receptor on the target cell. The viral spike glycoprotein can be cleaved into S1 and S2 domains (Bergeron et al., 2005; Du et al., 2007; Follis et al., 2006; Huang et al., 2006; Jackwood et al., 2001; Kawase et al., 2009; Watanabe et al., 2008; Yamada et al., 1998). The S1 domain of the viral spike protein dictates tropism and is responsible for mediating receptor binding (Chen et al., 1997; Han et al., 2007; Hensley and Baric, 1998; Hofmann et al., 2006; Lewicki and Gallagher, 2002; Li et al., 2003, 2007; Schultze et al., 1996; Thorp and Gallagher, 2004; Wentworth and Holmes, 2001). The S2 domain is responsible for mediating membrane fusion between the virus and host cell, with strong sequence conservation within the family (Bosch et al., 2004; Chu et al., 2006)—hence the mechanics of fusion can be expected to be conserved across the *Coronaviridae*.

Based on structural similarities, the SARS-CoV S glycoprotein is a class 1 membrane fusion protein (Schibli and Weissenhorn, 2004). The S2 domain contains two heptad repeat regions, HR1 and HR2, as well as a fusion peptide. Following conformational changes based on receptor binding or change in pH, the S2 domain drives fusion of the viral and host cell membranes to allow virus entry. Observations of cell surface expressed SARS-CoV spike protein, indicated that most of the protein was not cleaved at the S1–S2 boundary and with at best limited cleavage possible (Song et al., 2004; Xiao et al., 2003). It is generally considered that S1–S2 cleavage is not directly linked to fusion peptide exposure in the case of SARS-CoV, or any other coronavirus (Bosch and Rottier, 2008). However, it has recently been shown that SARS-CoV S can be proteolytically cleaved at a downstream position in S2, at residue 797 (Belouzard et al., 2009), and a highly conserved region C-terminal to the cleavage site has been characterized and identified as critical for fusion (Madu et al., 2009).

Downstream of these conserved core residues we observed another set of conserved residues flanked by cysteines 822 and 833. These flanks represent two of the 39 cysteines in S that are likely to form intra-disulfide bonds within S. Cysteine residues and their roles in mediating entry either in the receptor binding region or in the cytoplasmic tail have been well documented for coronaviruses (Petit et al., 2007; Petit et al., 2005; Thorp et al., 2006; Ye et al., 2004). For other families of viruses, cysteine residues have been key players for driving entry (Matthias and Hogg, 2003; Matthias et al., 2002) and fusion (Delos et al., 2008; Delos and White, 2000; Parrott et al., 2009; Rai et al., 2004). In this study, we investigated the importance of a conserved domain in SARS-CoV S2 flanked by cysteines 822 and 833 by carrying out a comprehensive mutagenesis study. Using cell–cell

* Corresponding author. Fax: +1 607 253 3385.
E-mail address: grw7@cornell.edu (G.R. Whittaker).

0042-6822/$ – see front matter © 2009 Elsevier Inc. All rights reserved.
doi:10.1016/j.virol.2009.07.038

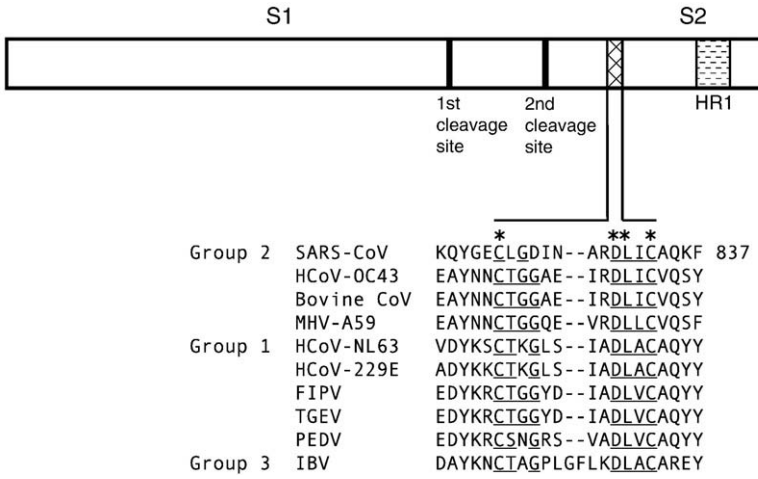

Fig. 1. Schematic and alignment of the cysteine-flanked region. A schematic representation of the coronavirus spike with hallmark domains alongside the region of interest. A multiple sequence alignment of the S protein from representative coronavirus groups was performed. Residues that are conserved directly or in terms of properties are underlined and asterisked residues represent 100% conservation within the CoV family. Virus abbreviations and Genbank accession numbers are as follows: SARS-CoV, accession no. AAP13441; HCoV-NL63, Human coronavirus NL63 Amsterdam accession no. AAS58177; HCoV-229E, Human coronavirus 229E accession no. AAG48592; HCoV-OC43, Human coronavirus OC43 ATCC VR-759 accession no. AAR01015; IBV, Infectious Bronchitis virus Beaudette strain accession no. AAY24433; MHV-A59, Mouse Hepatitis virus A59 accession no. AAB86819; PEDV, Porcine epidemic diarrhea virus LZC accession no. ABM64776; Bovine CoV, Bovine coronavirus R-AH187 accession no. ABP38295; ABP87990; FIPV, Feline infectious peritonitis virus WSU 79-1146 accession no. YP239355; TGEV, Transmissible gastroenteritis virus Purdue PUR46-MAD accession no. NP058424.

fusion and pseudovirus assays, we show that this domain is critical for the activation of SARS-CoV S-mediated membrane fusion and virus entry.

Results

Bioinformatic analysis of the SARS-CoV S2 domain flanked by cysteine residues C822 and C833

A common feature of regions within a viral glycoprotein that are required for entry is that they show a high degree of conservation within a virus family. We therefore performed a multiple sequence alignment of the spike protein of representative coronaviruses, with a focus on the domain flanked by cysteine residues C822 and C833. This bioinformatic analysis confirmed a high degree of conservation in the region (Fig. 1). Indeed, residues C822, D830, L831, and C833 of the SARS-CoV S represent some of the most conserved residues in that region and across the *Coronaviridae*.

Cloning and expression of WT and mutant SARS-CoV S glycoproteins

To test the fusogenic properties of the conserved S2 domain flanked by cysteine residues C822 and C833 a series of mutations were introduced into a SARS-CoV S protein-expressing vector to generate the following mutants: C822S, G824A, D825A, N827A, A828S, D830L, L831D, C833S, a double cysteine mutant (C822S/C833S), a deletion of the residues between the cysteines (Δ823–832) and a Gly-Ala-Gly (GAG) loop mutant to replace the residues between the cysteines. The rationale for these mutations was as follows: residues G824, D825, N827, and A828 were simply mutated to alanine (or serine in the case of A828) to modify their chemical nature in an innocuous manner; the conserved residues C822 and C833 were mutated to serine to change the chemical nature of the cysteines and prevent normal disulphide bond formation; the C822S/C833S double mutant was designed to curb the possibility of spurious disulfide bonding occurring with unpaired cysteines; D830L and L831D mutants were generated to modify the chemistry of each original residue with the corresponding conserved residue, as both are 100% conserved; and to further address how residues within the proposed loop might be important, we generated a loop deletion mutant Δ823–832 and a flexible tripeptide GAG loop (Kwong et al., 1998) between the flanking cysteines.

In order to evaluate the effect of the mutations on the fusogenic properties of SARS-CoV S protein, we first verified the cell surface expression of the mutants. The level of surface expression of the point mutants was verified quantitatively after transfection of expression vectors bearing mutant or wild type S protein in BHK-21 cells, at both 37 °C and 32 °C, followed by biotinylation and immunoblotting. At 37 °C, with the exception of the N827A mutant, we observed a tolerable surface expression of many of the mutants (Fig. 2A), but at 32 °C we observed an overall better surface expression of all mutants expressing at >65% of wild type levels (Fig. 2B) so this temperature was used in the corresponding surface expression fusion assays as well as in the generation of pseudotyped virions.

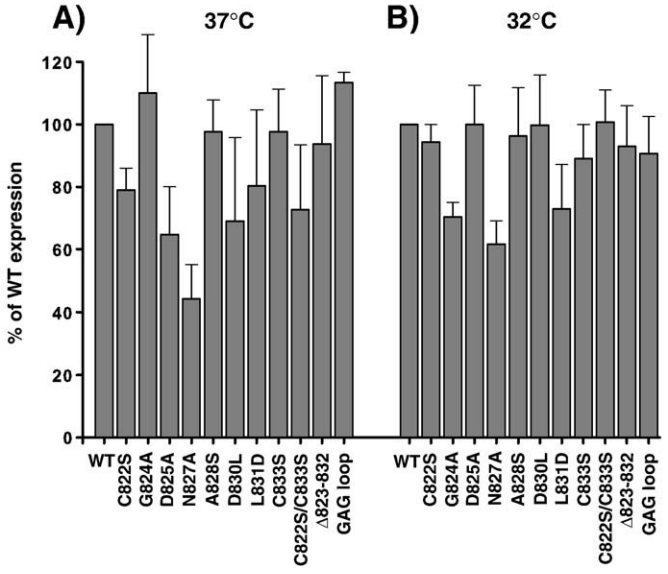

Fig. 2. Effect of point mutants on spike protein surface expression. BHK cells were transfected with plasmids encoding wild type SARS-CoV S or alanine mutants at either 37 °C (panel A) or 32 °C (panel B). The cells were labeled with Sulfo-NHS-SS-biotin and lysed. Lysates were affinity purified with NeutraAvidin beads and resolved by SDS-PAGE and Western blot using anti C9 tag antibody. The biotinylation assay was repeated three times and the results from the Western blots were quantified using IP lab software and plotted in Sigma Plot 9.0. Error bars represent standard deviation of the mean.

Binding of soluble hACE2-Fc to wild type or mutant SARS-CoV S

With point mutants introduced into the viral glycoprotein, it was important to confirm that the binding to ACE2 the SARS-CoV receptor is not altered. To confirm this, we cotransfected 293T cells with a construct expressing human ACE2 fused to the Fc-binding domain of human IgG (hACE2-Fc) and wild type or mutant spike vectors. 48 h post transfection, cells were lysed and affinity purified for hACE2-Fc, and then immunoblotted for SARS-CoV S to confirm interactions between receptor and spike. The levels of binding were observed to be comparable, with all mutants binding ACE2 at an average of >70% of wild type levels (Fig. 3).

Fusion assays of cells expressing WT or mutant SARS-CoV S and ACE2

With a tolerable level expression at the cell surface verified, we were then able to evaluate how the mutations might affect membrane fusion. Taking advantage of trypsin as a fusion trigger for the spike protein, we employed a quantitative method of determining SARS-CoV S protein-mediated membrane fusion activity, by using a luciferase-based assay system to measure cell–cell fusion. In this assay, BHK-21 cells were cotransfected with wild type or mutant spike protein along with T7 polymerase-driven luciferase gene and overlayed with Vero E6 cells transfected with the T7 polymerase gene. Fusion was induced by trypsin treatment, and the degree of luciferase activity after induction of fusion was used as an indicator of the fusogenic ability of the mutant SARS-CoV S protein, in comparison to wild type (Fig. 4). We observed that while alanine substitution of less conserved residues G824A, D825A, N827A, and A828S, displayed activity close to or better than wild type, mutation of the core-conserved residues, as well as the loop deletion and mini-loop mutants resulted in luciferase activity that was close to background levels in comparison to wild type activity.

Characterization of SARS-CoV S mutants in MLV-pseudotyped virions

To better understand the roles of S2 domain flanked by cysteine residues C822 and C833 in the context of a virus particle, we employed a retrovirus-based pseudovirion system (Bartosch et al., 2003). In this infectivity assay, 293T cells are first cotransfected with a murine leukemia virus (MLV) Gag-Pol and luciferase plasmid along with either the SARS-CoV wild type or mutant S protein plasmid, or with an empty vector control, to generate control-pseudotyped viral particles. The transfected cells were then incubated for 72 h at 32 °C, as this temperature was optimal for surface expression of the mutants. We first confirmed that a suitable level of expression of mutant spike protein was incorporated in the viral particles, in comparison to wild type, by blotting for spike protein in the collected supernatant 72 h post transfection (Fig. 5). Although mutant N827A showed a low level

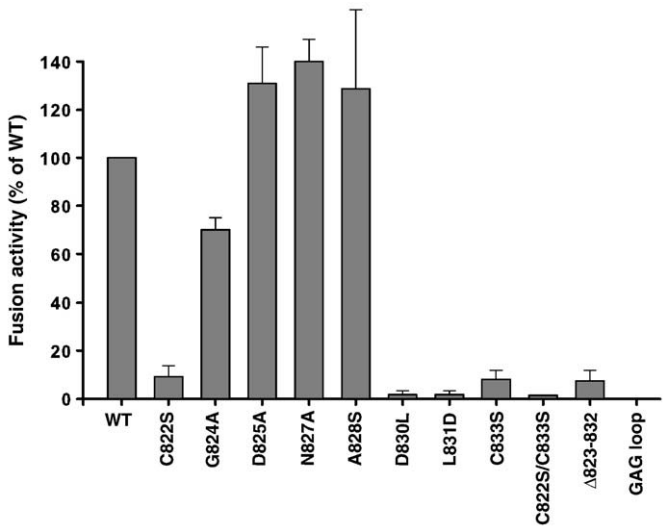

Fig. 4. Quantitative assays of membrane fusion mediated by mutant spike proteins. BHK cells were cotransfected with plasmids encoding wild type SARS-CoV S or alanine mutants and also with luciferase cDNA under the control of a T7 promoter. At 24 h post transfection, BHK cells were then overlaid with Vero cells previously transfected with a plasmid encoding T7 polymerase. After 3 h, fusion was induced using media containing 2 μg/ml trypsin. The cells were lysed 6 h post fusion induction and supernatants measured for luciferase activity. Each bar is averaged from three individual repeats and error bars represent standard deviation from the mean.

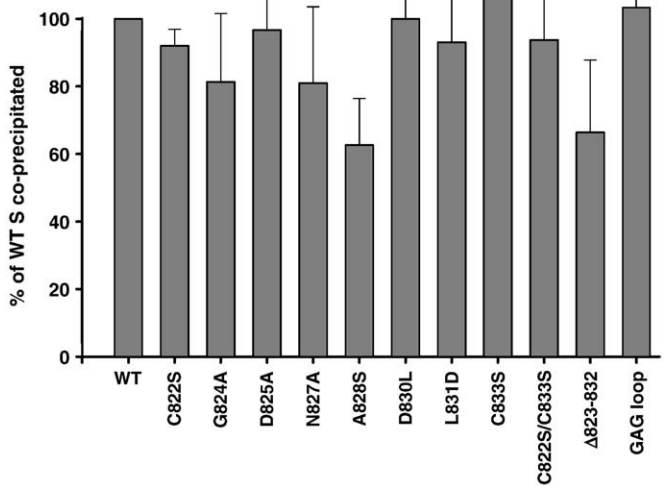

Fig. 3. Effect of point mutants on receptor binding. 293T cells were grown on 6 cm dishes and cotransfected with plasmids expressing wild type or mutant spike protein and human ACE2-Fc. The cells were lysed and the lysates were affinity purified using immobilized Protein A beads. Protein A beads were then washed and resolved via SDS-PAGE and Western blot. The binding assay was repeated three times and results from the Western blot quantifications were plotted using Sigma Plot 9.0 (Systat Software).

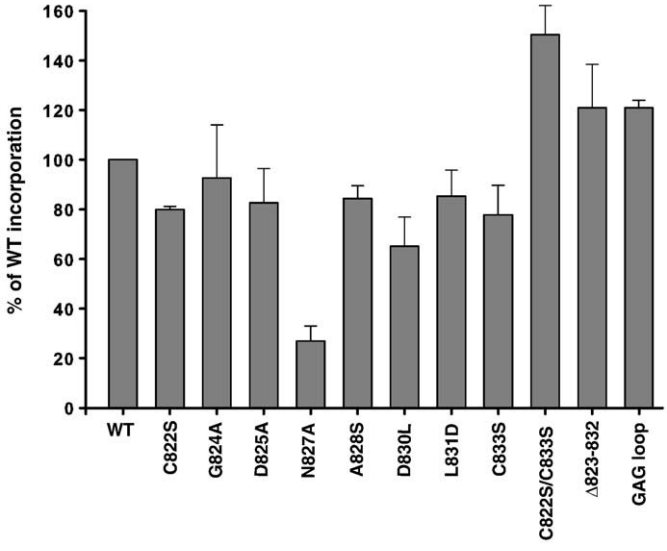

Fig. 5. Incorporation of mutant spike proteins into MLV-pseudotyped virions. Spike protein–MLV-pseudotyped virions were prepared as described in the Materials and methods. Virions were concentrated using a 10% PEG precipitation, diluted in SDS sample buffer, and resolved by SDS-PAGE and Western blot using a monoclonal antibody specific for the C9 tag. The spike protein–MLV-pseudotyped virions were generated three times for wild type or mutants, and the results from the Western blots were quantified using IP lab software and plotted in Sigma Plot 9.0. Error bars represent standard deviation from the mean.

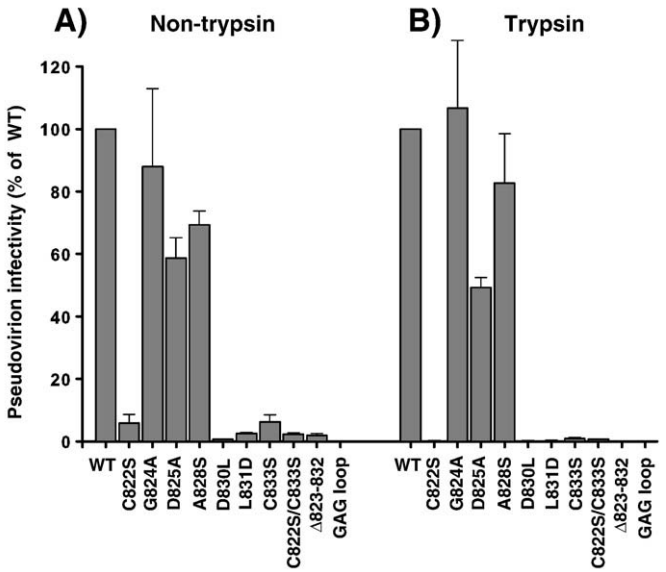

Fig. 6. Infectivity of spike protein–MLV-pseudotyped virions. (A) Endosomal (non-trypsin-mediated) infectivity of spike protein–MLV-pseudotyped virions. Virions were bound to Vero cells at 4 °C in RPMI media for 2 h. After binding, cells were rinsed in RPMI media before being replaced with complete DMEM and incubated at 37 °C. 48 h post-binding cells were lysed and assayed for luciferase activity. Each bar is averaged from three individual infectivity assays and error bars represent standard deviation of the mean. (B) Trypsin-mediated infectivity of spike protein–MLV-pseudotyped virions. Virions were bound to Vero cells at 4 °C in RPMI media and treated with 25 mM ammonium chloride. Fusion was induced using serum-free media containing 2 μg/ml trypsin. The cells were lysed 48 h post fusion induction and supernatants assayed for luciferase activity. Each bar is averaged from three individual infectivity assays and error bars represent standard deviation of the mean.

of spike incorporation, the other mutants expressing at levels greater than 60% of the wild type the level of cell surface expression in 293T was also confirmed by our biotinylation assay (data not shown). Upon confirmation of mutant spike protein incorporation, Vero E6 cells were then transduced with SARS-CoV S pseudovirions with comparable levels of detected spike by adjusting the volume of the supernatant to ensure that equal amounts of S protein were used in the infectivity assay. At 48 h post transduction, cells were lysed and luciferase activity measured as an indicator of the extent of viral infection. The luciferase activity of the wild type was set to 100% and luciferase activities of the mutants were normalized to wild type. As shown in Fig. 6A, we observed a pattern that was similar to the quantitative cell–cell fusion data (see Fig. 4) although the level activity of the D825A mutant is at an average of about 70% of the WT.

It is considered that SARS-CoV has the ability to fuse in both endocytic and non-endocytic compartments, and as such we assessed any potential differences in the role of this cysteine-flanked region in each of these two pathways of virus entry. We therefore inhibited infection by the endocytic route using the lysosomotropic base NH_4Cl, and induced fusion of surface-bound virions by trypsin activation. At 48 h post trypsin treatment, cells were assayed for luciferase activity. We observed that in this assay of non-endosomal infection that the overall results reflect both trypsin-untreated assay and the cell–cell fusion data (Fig. 6B).

Discussion

The coronavirus spike protein is responsible for mediating both the attachment and fusion that is required to deliver the viral genome. Binding of the virus to the host cell receptor sets in motion a series of rearrangements of the fusion protein in preparation for fusion. The fusion event as directed by the S2 domain requires a concerted cooperation within the domains of the fusion protein. In this study, we describe a conserved region essential to the S2 function of fusing host and viral membrane.

It has been recently published that a critical cleavage event at R797 occurs in SARS-CoV S (Belouzard et al., 2009), which might expose a viral fusion peptide (Madu et al., 2009). 25 residues C-terminal to the cleavage site, we observed an interesting conserved domain flanked by cysteine residues C822 and C833. Given its proximity to a cleavage site and the proposed fusion peptide, we set out to characterize this domain. Sequence alignment of this domain showed a strong conservation particularly in the C-terminus of the region. We set out to carry out a series of mutagenic studies in a comprehensive manner. Our investigation entailed the replacing of core-conserved residues with residues to modify the chemistry of the wild type residues, and substituting or deleting the residues between the

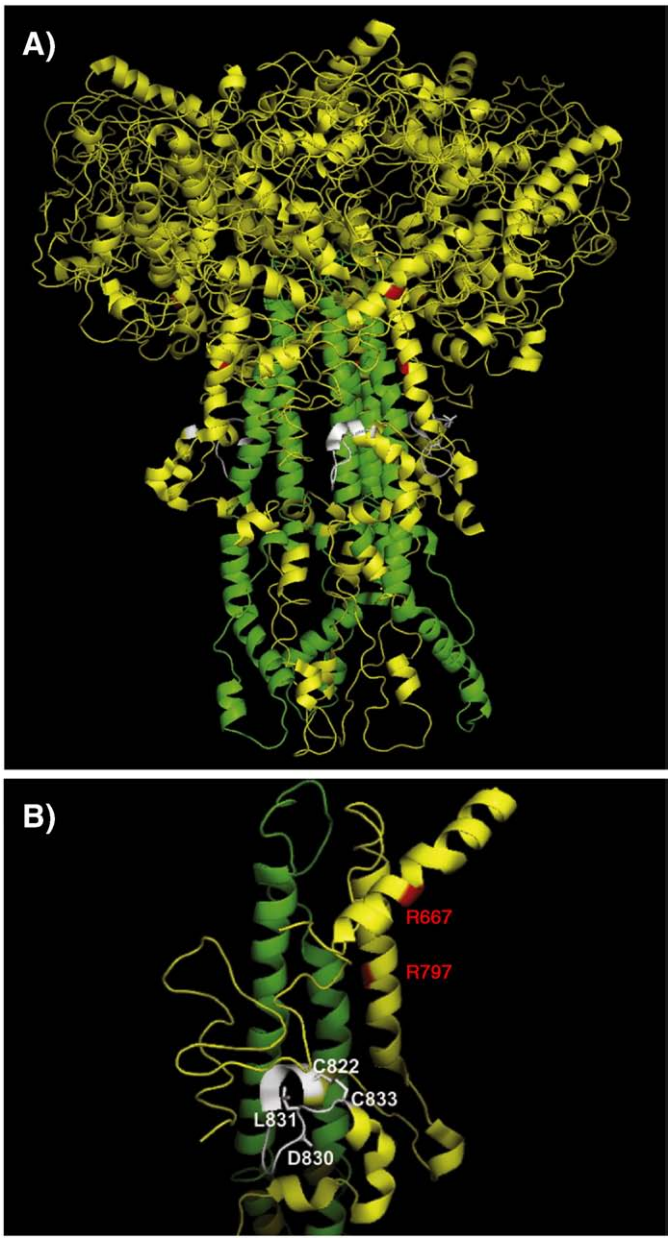

Fig. 7. Predicted structural model of the cysteine-flanked region. (A) A three dimensional model of the SARS-CoV S protein ectodomain trimer is shown in cartoon form, based on PDB file 1T7G. The figure was generated in MacPyMOL (DeLano Scientific), with the cysteine-flanked region colored white, both the S1 and S2 cleavage sites (R667 and R797) colored red and HR1 in green. (B) A monomer of the spike depicting the environment of the cysteine-flanked region. The side chains of conserved residues C822, D830, L831 and C822 are shown.

cysteines. This comprehensive investigation of the residues between C822 and C833 allowed us to gauge the extent of involvement of this region in the membrane fusion process. In all cases, we observed very limited to no effects on either surface expression or receptor binding, but observed drastic loss in fusogenic ability in the mutants of the core-conserved residues, in comparison to the wild type SARS-CoV S in cell–cell fusion assays.

In the context of a virus particle, we generated MLV-pseudovirions containing either WT or mutant S proteins. The mutant proteins were found to incorporate into MLV-pseudovirions at a level suitable for assessment of S function during virus entry. Upon pseudoparticle transduction, a drastic loss in the ability to infect cells was observed for both "endosomal" and "non-endosomal" routes of infection. The manner of sensitivity for these MLV-S mutants was very similar to the cell–cell fusion data thus indicating the importance of this region for fusion.

We hypothesize that this region acts as a means of relaying the signal for fusion activation within the subunit of S2, presumably based on conformational changes induced by low pH and/or receptor binding. One possible way the domain flanked by cysteine residues C822 and C833 may do so is by forming a disulfide bond-anchored loop that interacts with an as yet undisclosed part of the fusion protein to promote membrane fusion. In the absence of a crystal structure of the SARS-CoV S ectodomain, a predictive model of the quaternary structure is available: PDB code 1T7G (Bernini et al., 2004; Spiga et al., 2003) (Fig. 7A). In the context of this model, the cysteine-flanked region is represented as a loop region with the cysteines 822 and 833 positioned directly next to each other, which we predict to form a disulphide bond (Fig. 7B). The environment is one that might hint at further interactions with other parts of the spike protein. Of particular interest is the finding that residues C822, L823, G824, D825, I826, N827 and A828 within the loop are part of a major antigenic determinant of SARS-CoV S (residues L803–A828) capable of inducing neutralizing antibodies (Zhang et al., 2004). In conclusion, we present data of a critical domain of SARS-CoV S2 that is required for the successful function of S-mediated fusion. We propose this region functions by interactions with other domain(s) in S to activate membrane fusion. It is important to point out that in the absence of a "true" crystal structure, we cannot rule out the fact that this region may function through many other possible roles within SARS-CoV S to aid in membrane fusion.

Materials and methods

Cell culture

BHK-21, Vero E6 and 293T cells obtained from the American Type Culture Collection were used in this study. All cells were maintained in Dulbecco's modified Eagle's medium (DMEM, Cellgro) containing 10% fetal bovine serum, 100 U/ml penicillin and 10 μg/ml streptomycin (complete DMEM).

Generation of mutant SARS-CoV spike glycoproteins

Site-directed mutagenesis was carried out on the spike protein-expressing vector pcDNA3.1-SARS-CoV S (kindly provided by Dr. Michael Farzan, New England Primate Research Center) via PCR, using primers obtained from IDT technologies. Mutations were then confirmed by sequencing using an Applied Biosystems Automated 3730 DNA Analyzer at the Cornell University Life Sciences Core Laboratories Center.

Analysis of SARS-CoV S cell surface expression

BHK-21 cells were grown on 6 well plates and transfected with 1 μg of wild type or mutant spike protein-expressing plasmids using Lipofectamine 2000 (Invitrogen) for 36 h at 32 °C. Transfected cells were washed twice with cold phosphate buffered saline (PBS) and then labeled with 250 μg/ml Sulfo-NHS-SS-biotin (Pierce) for 30 min on ice. 50 mM cold glycine solution was added to the cells three times at 5 min intervals to quench unlabelled free biotin followed by a PBS wash. The cells were lysed in 500 μl of lysis buffer (Tris-buffered saline (TBS) containing 1% NP-40 and complete protease inhibitor mixture (Roche Applied Science)). The lysates were affinity purified using immobilized NeutraAvidin beads (Pierce) overnight at 4 °C. NeutraAvidin beads were then washed with lysis buffer followed by addition of SDS-PAGE sample loading buffer containing 100 mM dithiothreitol. The surface expression was analyzed by Western blot using the anti-C9 epitope tag monoclonal antibody Rho 1D4 (National Cell Culture Center, Minneapolis MN) and images were obtained and quantified using a LAS-3000 mini Fuji film imaging system and software (Fuji Photo Film Co., Ltd.). The biotinylation assay was repeated three times and results from the Western blot quantifications were plotted using Sigma Plot 9.0 (Systat Software).

Human ACE2-Fc-binding assay

293T cells were grown on 6 cm dishes and cotransfected with 2 μg each of wild type or mutant spike protein-expressing plasmids and human ACE2-Fc expressing plasmids using Lipofectamine 2000 (Invitrogen) for 48 h at 32 °C. Transfected cells were washed with cold phosphate buffered saline (PBS) and the cells were lysed in 500 μl of lysis buffer (Tris-buffered saline (TBS) containing 1% CHAPS and complete protease inhibitor mixture (Roche Applied Science)). The lysates were affinity purified using immobilized Protein A beads (Pierce) overnight at 4 °C. Protein A beads were then washed three times with 0.5% CHAPS lysis buffer followed by addition of SDS-PAGE sample loading buffer containing 100 mM dithiothreitol. The SARS-CoV S binding to precipitated ACE2-Fc was analyzed by Western blot using the anti-C9 epitope tag monoclonal antibody Rho 1D4 (National Cell Culture Center, Minneapolis MN) and images were obtained and quantified using a LAS-3000 mini Fuji film imaging system and software (Fuji Photo Film Co., Ltd.). The binding assay was repeated three times and results from the Western blot quantifications were plotted using Sigma Plot 9.0 (Systat Software).

Quantitative cell–cell fusion assay

BHK-21 cells were grown in 24 well plates and cotransfected with wild type or mutant spike protein-expressing plasmids and a plasmid encoding luciferase under the control of a T7 promoter, using Lipofectamine 2000 (Invitrogen) for 24 h at 32 °C. Vero E6 cells in a 60 mm dish were also transfected with a plasmid encoding the T7 polymerase. After 24 h the BHK-21 cells were overlaid with Vero E6 cells and incubated for 3 h. Cells were treated with serum-free media containing 2 μg/ml trypsin to induce fusion and replaced with complete DMEM after 30 min. At 6 h post induction, cells were lysed and assayed for Luciferase activity using a Luciferase assay kit (Promega) and a Glomax 20/20 luminometer (Promega) to measure light emission.

Spike protein-pseudotyped virion production

Pseudotyped virions were generated using plasmids kindly provided by Dr. Jean Dubuisson (Lille Pasteur Institute, France). 293T cells were cotransfected with a murine leukemia virus (MLV)-based transfer vector encoding luciferase, a MLV Gag-Pol packaging construct and a pcDNA3.1-SARS-CoV S plasmid encoding wild type or mutant spike envelope glycoprotein, using Exgen 500 (Fermentas) as recommended. After incubation for 72 h at 32 °C, supernatants were collected and filtered through a 0.45 μm pore size membrane. The level of spike protein incorporation was confirmed by polyethylene

glycol (PEG) concentration, centrifugation and Western blot analysis. 600 μl of filtered supernatant was mixed with 200 μl 40% PEG and centrifuged for 30 min at 4000 rpm at 4 °C. The pellet was redissolved in SDS-PAGE sample loading buffer containing 100 mM dithiothreitol and blotted in the same manner as described above in the cell surface biotinylation assay.

Spike protein-pseudotyped virion infectivity assays

Equal levels of pseudoparticles were used based on the level of spike protein-pseudotype virions quantified by Western blot, as described above. For a typical infection assay, spike protein-pseudotyped virions containing wild type or mutant glycoproteins were bound for 2 h in RPMI media containing 0.2% BSA, 20 mM HEPES to Vero E6 cells at 4 °C. Media was exchanged for complete DMEM and incubated for 48 h at 37 °C. The cells were then lysed and luciferase activity measured using the same methods as the quantitative cell–cell fusion assay. In a trypsin-mediated cell surface infectivity assay, Vero E6 cells were first pre-incubated with 25 mM NH_4Cl for 1 h at 37 °C. Pseudotyped virions were then bound for 2 h in RPMI media containing 0.2% BSA, 20 mM HEPES, and 25 mM NH_4Cl at 4 °C. The cells were then warmed up with the addition of pre-warmed RPMI media containing 5 μg/ml trypsin, 0.2% BSA, 20 mM HEPES, and 25 mM ammonium chloride for 5 min at 37 °C in a water bath.

Acknowledgements

We thank Ruth Collins and all members of the Whittaker laboratory for helpful discussions and input during the course of this work and Michael Farzan, Tom Gallagher and Jean Dubuisson for their kind provision of reagents. I.G.M. was the recipient of a fellowship from the National Institutes of Health (NIGMS), grant F31 GM082084. Work in the author's laboratory was also supported by National Institutes of Health (NIAID) grants R03 AI060946 and R21 AI1076258.

References

Bartosch, B., Dubuisson, J., Cosset, F.L., 2003. Infectious hepatitis C virus pseudo-particles containing functional E1–E2 envelope protein complexes. J. Exp. Med. 197 (5), 633–642.

Belouzard, S., Chu, V.C., Whittaker, G.R., 2009. Activation of the SARS coronavirus spike protein via sequential proteolytic cleavage at two distinct sites. Proc. Natl. Acad. Sci. U. S. A. 106 (14), 5871–5876.

Bergeron, E., Vincent, M.J., Wickham, L., Hamelin, J., Basak, A., Nichol, S.T., Chretien, M., Seidah, N.G., 2005. Implication of proprotein convertases in the processing and spread of severe acute respiratory syndrome coronavirus. Biochem. Biophys. Res. Commun. 326 (3), 554–563.

Bernini, A., Spiga, O., Ciutti, A., Chiellini, S., Bracci, L., Yan, X., Zheng, B., Huang, J., He, M.L., Song, H.D., Hao, P., Zhao, G., Niccolai, N., 2004. Prediction of quaternary assembly of SARS coronavirus peplomer. Biochem. Biophys. Res. Commun. 325 (4), 1210–1214.

Bosch, B.J., Rottier, P.J., 2008. Nidovirus entry into cells. In: Perlman, S., Gallagher, T., Snijder, E.J. (Eds.), Nidoviruses. ASM Press, Washington DC, pp. 157–178.

Bosch, B.J., Martina, B.E.E., van der Zee, R., Lepault, J., Haijema, B.J., Versluis, C., Heck, A.J.R., de Groot, R., Osterhaus, A., Rottier, P.J.M., 2004. Severe acute respiratory syndrome coroavirus (SARS-CoV) infection inhibition using spike protein heptad repeat-derived peptides. Proc. Natl. Acad. Sci. U. S. A. 101 (22), 8455–8460.

Chen, D.S., Asanaka, M., Chen, F.S., Shively, J.E., Lai, M.M.C., 1997. Human carcinoembryonic antigen and biliary glycoprotein can serve as mouse hepatitis virus receptors. J. Virol. 71 (2), 1688–1691.

Chu, V.C., McElroy, L.J., Chu, V., Bauman, B.E., Whittaker, G.R., 2006. The avian coronavirus infectious bronchitis virus undergoes direct low-pH-dependent fusion activation during entry into host cells. J. Virol. 80 (7), 3180–3188.

Delos, S.E., White, J.M., 2000. Critical role for the cysteines flanking the internal fusion peptide of avian sarcoma/leukosis virus envelope glycoprotein. J. Virol. 74 (20), 9738–9741.

Delos, S.E., Brecher, M.B., Chen, Z.Y., Melder, D.C., Federspiel, M.J., White, J.M., 2008. Cysteines flanking the internal fusion peptide are required for the avian sarcoma/leukosis virus glycoprotein to mediate the lipid mixing stage of fusion with high efficiency. J. Virol. 82 (6), 3131–3134.

Drosten, C., Gunther, S., Preiser, W., van der Werf, S., Brodt, H.R., Becker, S., Rabenau, H., Panning, M., Kolesnikova, L., Fouchier, R.A.M., Berger, A., Burguiere, A.M., Cinatl, J., Eickmann, M., Escriou, N., Grywna, K., Kramme, S., Manuguerra, J.C., Muller, S., Rickerts, V., Sturmer, M., Vieth, S., Klenk, H.D., Osterhaus, A., Schmitz, H., Doerr, H.W., 2003. Identification of a novel coronavirus in patients with severe acute respiratory syndrome. New Engl. J. Med. 348 (20), 1967–1976.

Du, L.Y., Kao, R.Y., Zhou, Y.S., He, Y.X., Zhao, G.Y., Wong, C., Jiang, S.B., Yuen, K.Y., Jin, D.Y., Zheng, B.J., 2007. Cleavage of spike protein of SARS coronavirus by protease factor Xa is associated with viral infectivity. Biochem. Biophys. Res. Commun. 359 (1), 174–179.

Follis, K.E., York, J., Nunberg, J.H., 2006. Furin cleavage of the SARS coronavirus spike glycoprotein enhances cell–cell fusion but does not affect virion entry. Virology 350 (2), 358–369.

Fouchier, R.A.M., Kuiken, T., Schutten, M., van Amerongen, G., van Doornum, J., van den Hoogen, B.G., Peiris, M., Lim, W., Stohr, K., Osterhaus, A., 2003. Aetiology — Koch's postulates fulfilled for SARS virus. Nature 423 (6937), 240.

Han, D.P., Lohani, M., Cho, M.W., 2007. Specific asparagine-linked glycosylation sites are critical for DC-SIGN- and L-SIGN-mediated severe acute respiratory syndrome coronavirus entry. J. Virol. 81 (21), 12029–12039.

Hensley, L.E., Baric, R.S., 1998. Human biliary glycoproteins function as receptors for interspecies transfer of Mouse Hepatitis virus. In: Enjuanes, L., Siddell, S.G., Spaan, W. (Eds.), Coronaviruses and Arteriviruses, Vol. 440, pp. 43–52.

Hofmann, H., Simmons, G., Rennekamp, A.J., Chaipan, C., Gramberg, T., Heck, E., Geier, M., Wegele, A., Marzi, A., Bates, P., Pohlmann, S., 2006. Highly conserved regions within the spike proteins of human coronaviruses 229E and NL63 determine recognition of their respective cellular receptors. J. Virol. 80 (17), 8639–8652.

Holmes, K.V., 2003. SARS-associated coronavirus. New Engl. J. Med. 348 (20), 1948–1951.

Huang, I.C., Bosch, B.J., Li, F., Li, W.H., Lee, K.H., Ghiran, S., Vasilieva, N., Dermody, T.S., Harrison, S.C., Dormitzer, P.R., Farzan, M., Rottier, P.J.M., Choe, H., 2006. SARS coronavirus, but not human coronavirus NL63, utilizes cathepsin L to infect ACE2-expressing cells. J. Biol. Chem. 281 (6), 3198–3203.

Jackwood, M.W., Hilt, D.A., Callison, S.A., Lee, C.W., Plaza, H., Wade, E., 2001. Spike glycoprotein cleavage recognition site analysis of infectious bronchitis virus. Avian Dis. 45 (2), 366–372.

Kawase, M., Shirato, K., Matsuyama, S., Taguchi, F., 2009. Protease-mediated entry via the endosome of human coronavirus 229E. J. Virol. 83 (2), 712–721.

Kwong, P.D., Wyatt, R., Robinson, J., Sweet, R.W., Sodroski, J., Hendrickson, W.A., 1998. Structure of an HIV gp120 envelope glycoprotein in complex with the CD4 receptor and a neutralizing human antibody. Nature 393 (6686), 648–659.

Lewicki, D.N., Gallagher, T.M., 2002. Quaternary structure of coronavirus spikes in complex with carcinoembryonic antigen-related cell adhesion molecule cellular receptors. J. Biol. Chem. 277 (22), 19727–19734.

Li, W.H., Moore, M.J., Vasilieva, N., Sui, J.H., Wong, S.K., Berne, M.A., Somasundaran, M., Sullivan, J.L., Luzuriaga, K., Greenough, T.C., Choe, H., Farzan, M., 2003. Angiotensin-converting enzyme 2 is a functional receptor for the SARS coronavirus. Nature 426 (6965), 450–454.

Li, W.H., Sui, J.H., Huang, I.C., Kuhn, J.H., Radoshitzky, S.R., Marasco, W.A., Choe, H., Farzan, M., 2007. The S proteins of human coronavirus NL63 and severe acute respiratory syndrome coronavirus bind overlapping regions of ACE2. Virology 367 (2), 367–374.

Madu, I.G., Roth, S.L., Belouzard, S., Whittaker, G.R., 2009. Characterization of a highly conserved domain within the severe acute respiratory syndrome coronavirus spike protein S2 domain with characteristics of a viral fusion peptide. J. Virol. 83 (15), 7411–7421.

Matthias, L.J., Hogg, P.J., 2003. Redox control on the cell surface: implications for HIV-1 entry. Antioxid. Redox Signal. 5 (1), 133–138.

Matthias, L.J., Yam, P.T.W., Jiang, X.M., Vandegraaff, N., Li, P., Poumbourios, P., Donoghue, N., Hogg, P.J., 2002. Disulfide exchange in domain 2 of CD4 is required for entry of HIV-I. Nat. Immunol. 3 (8), 727–732.

Parrott, M.M., Sitarski, S.A., Arnold, R.J., Picton, L.K., Hill, R.B., Mukhopadhyay, S., 2009. Role of conserved cysteines in the alphavirus E3 protein. J. Virol. 83 (6), 2584–2591.

Petit, C.M., Melancon, J.M., Chouljenko, V.N., Colgrove, R., Farzan, M., Knipe, D.M., Kousoulas, K.G., 2005. Genetic analysis of the SARS-coronavirus spike glycoprotein functional domains involved in cell-surface expression and cell-to-cell fusion. Virology 341 (2), 215–230.

Petit, C.M., Chouljenko, V.N., Iyer, A., Colgrove, R., Farzan, M., Knipe, D.M., Kousoulas, K.G., 2007. Palmitoylation of the cysteine-rich endodomain of the SARS-coronavirus spike glycoprotein is important for spike-mediated cell fusion. Virology 360 (2), 264–274.

Rai, T., Marble, D., Rihani, K., Rong, L.J., 2004. The spacing between cysteines two and three of the LDL-A module of Tva is important for subgroup A avian sarcoma and leukosis virus entry. J. Virol. 78 (2), 683–691.

Schibli, D.J., Weissenhorn, W., 2004. Class I and class II viral fusion protein structures reveal similar principles in membrane fusion (Review). Mol. Membr. Biol. 21 (6), 361–371.

Schultze, B., Krempl, C., Ballesteros, M.L., Shaw, L., Schauer, R., Enjuanes, L., Herrler, G., 1996. Transmissible gastroenteritis coronavirus, but not the related porcine respiratory coronavirus, has a sialic acid (N-glycolylneuraminic acid) binding activity. J. Virol. 70 (8), 5634–5637.

Song, H.C., Seo, M.Y., Stadler, K., Yoo, B.J., Choo, Q.L., Coates, S.R., Uematsu, Y., Harada, T., Greer, C.E., Polo, J.M., Pileri, P., Eickmann, M., Rappuoli, R., Abrignani, S., Houghton, M., Han, J.H., 2004. Synthesis and characterization of a native, oligomeric form of recombinant severe acute respiratory syndrome coronavirus spike glycoprotein. J. Virol. 78 (19), 10328–10335.

Spiga, O., Bernini, A., Ciutti, A., Chiellini, S., Menciassi, N., Finetti, F., Causarono, V., Anselmi, F., Prischi, F., Niccolai, N., 2003. Molecular modelling of S1 and S2 subunits

of SARS coronavirus spike glycoprotein. Biochem. Biophys. Res. Commun. 310 (1), 78–83.
Thorp, E.B., Gallagher, T.M., 2004. Requirements for CEACAMs and cholesterol during murine coronavirus cell entry. J. Virol. 78 (6), 2682–2692.
Thorp, E.B., Boscarino, J.A., Logan, H.L., Goletz, J.T., Gallagher, T.M., 2006. Palmitoylations on murine coronavirus spike proteins are essential for virion assembly and infectivity. J. Virol. 80 (3), 1280–1289.
Watanabe, R., Matsuyama, S., Shirato, K., Maejima, M., Fukushi, S., Morikawa, S., Taguchi, F., 2008. Entry from the cell surface of severe acute respiratory syndrome coronavirus with cleaved S protein as revealed by pseudotype virus bearing cleaved S protein. J. Virol. 82 (23), 11985–11991.
Wentworth, D.E., Holmes, K.V., 2001. Molecular determinants of species specificity in the coronavirus receptor aminopeptidase N (CD13): influence of N-linked glycosylation. J. Virol. 75 (20), 9741–9752.
Xiao, X.D., Chakraborti, S., Dimitrov, A.S., Gramatikoff, K., Dimitrov, D.S., 2003. The SARS-CoV S glycoprotein: expression and functional characterization. Biochem. Biophys. Res. Commun. 312 (4), 1159–1164.
Yamada, Y.K., Takimoto, K., Yabe, M., Taguchi, F., 1998. Requirement of proteolytic cleavage of the murine coronavirus MHV-2 spike protein for fusion activity. In: Enjuanes, L., Siddell, S.G., Spaan, W. (Eds.), Coronaviruses and Arteriviruses, Vol. 440, pp. 89–93.
Ye, R., Montalto-Morrison, C., Masters, P.S., 2004. Genetic analysis of determinants for spike glycoprotein assembly into murine coronavirus virions: distinct roles for charge-rich and cysteine-rich regions of the endodomain. J. Virol. 78 (18), 9904–9917.
Zhang, H., Wang, G.W., Li, H., Nie, Y.C., Shi, X.L., Lian, G.W., Wang, W., Yin, X.L., Zhao, Y., Qu, X.X., Ding, M.X., Deng, H.K., 2004. Identification of an antigenic determinant on the S2 domain of the severe acute respiratory syndrome coronavirus spike glycoprotein capable of inducing neutralizing antibodies. J. Virol. 78 (13), 6938–6945.